

## Supporting Information

# Simultaneous antimicrobial and anticoagulant surfaces based on nanoparticles and polysaccharides

Doris Breitwieser<sup>a</sup>, Stefan Spirk<sup>b,c,\*</sup>, Hubert Fasl<sup>a</sup>, Heike M.A. Ehmann<sup>a,b</sup>, Angela Chemelli<sup>a</sup>, Victoria E. Reichel<sup>a</sup>, Christian Gspan<sup>d</sup>, Karin Stana-Kleinschek<sup>b</sup>, and Volker Ribitsch<sup>a</sup>

<sup>a</sup>Institute of Chemistry, University of Graz, Heinrichstrasse 28, 8010 Graz, Austria

<sup>b</sup>Institute for the Engineering of Materials and Design, Laboratory for Characterization and Processing of Polymers,

University of Maribor, Smetanova Ulica, 2000 Maribor, Slovenia

<sup>c</sup>Institute for Chemistry and Technology of Materials, University of Technology Graz, Stremayrgasse 9, 8010 Graz, Austria.

<sup>d</sup>Institute for Electron Microscopy and Fine Structure Research, Centre for Electron Microscopy Graz, Steyrergasse 17, 8010 Graz, Austria.

**\*To whom correspondence should be addressed: [stefan\\_spirk@yahoo.de](mailto:stefan_spirk@yahoo.de), Tel:**

**+38622207947, Fax: +38622207996**

## Experimental Details

### *Fehling Test*

Fehling I (2 ml, 8.4 mmol) and Fehling II (2 ml, 8.7 mmol) solutions were mixed and S-Chi (4 mg, 0.017 mmol) was added. The mixture was carefully heated with a Bunsen burner, and a brick red precipitation was observed along with a decolorization of the blue solution.

### *UV-VIS Spectroscopy*

The UV-VIS measurements of AgNP aqueous solutions were performed on a Varian Cary 50. For the elucidation of the mechanism of formation, S-Chi concentration was varied and a clear decrease in absorption could be observed in the UV-VIS (**Fig. S1**).

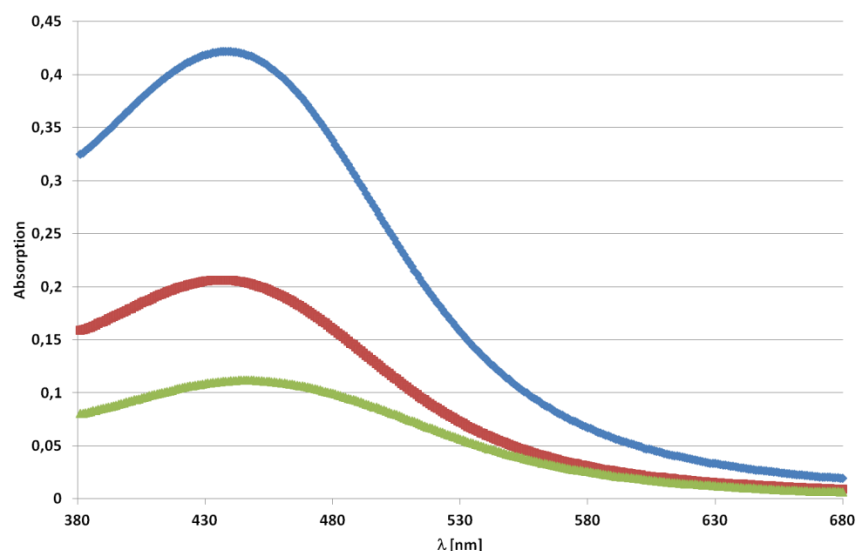


**Figure S1.** Silver nanoparticle formation in dependence of the S-Chi concentration monitored by UV VIS spectroscopy. The silver level was kept constant according to the main manuscript. Blue: 1 mg/ ml, red 0.5 mg/ml, green 0.25 mg/ml S-Chi. A slight shifting of the plasmon resonance can be observed with lower S-Chi concentrations.

### *Fluorescence spectroscopy and fluorescence labeling with 6-aminofluorescein (AF)*

Fluorescence spectroscopy was done on a Varian Eclipse using 490 nm as excitation wavelength.

For fluorescent experiments, S-Chi (5 mg, 0.021 mmol) was dissolved in 2 ml 0.5 M KCl (sample A). For sample B, 100  $\mu$ l ethylenediamine (0.90 g, 1.7 mmol) were added to this solution to block the aldehyde functionality of S-Chi and stirred for one hour at room

temperature. To both samples 250  $\mu$ l of an aqueous 6-aminofluorescein solution ( $c=1.4$   $\mu$ mol/ml) were added and stirred for one hour. Afterwards chromatography (using GE healthcare PD 10 desalting columns) was performed to remove trace amounts of AF. As expected, sample A showed fluorescence with an excitation maximum at 515 nm (typically for 6-aminofluorescein), while sample B did not exhibit any fluorescence (**Fig. S2**).

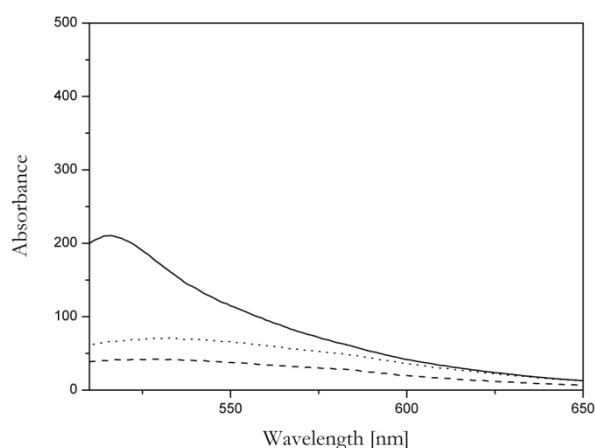


**Figure S2.** Fluorescence emission spectra (excitation wavelength 495 nm) of different samples. --- S-Chi with ethylenediamine, •••S-Chi with ethylenediamine and 6-aminofluorescein. Full line: S-Chi with 6-aminofluorescein.

### *Transmission Electron Microscopy (TEM)*

Bright field images were acquired on a Tecnai F20 transmission electron microscope with a Schottky Field Emission Gun (FEG) operating at 200 kV. The energy filtered images were recorded with a post column energy filter (Gatan Imaging Filter, GIF) on a  $2k \times 2k$  CCD. The samples were prepared by dispersing finely ground material onto a holey carbon film.

### *Small angle X-ray scattering*

The SAXS equipment used consists of a SAXSess camera (Anton-Paar, Graz, Austria) connected to an X-ray generator (Philips, PW1730/10) operating at 40 kV and 50 mA with a sealed-tube Cu anode. The divergent polychromatic X-ray beam was focused into a line shaped beam of Cu  $K_{\alpha}$  radiation ( $\lambda = 0.154$  nm) with a Goebel mirror. A PI-SCX fused fiber

optic taper CCD camera from Princeton Instruments (Trenton, NJ, USA) was used to record the two-dimensional scattering patterns. It has a 2084×2084 array with 24 μm × 24 μm pixel size (chip size: 50 mm×50 mm). The CCD detector was operated at -30 °C.

Capillaries were filled with aqueous solutions of the AgNPs and placed in the sample holder. Measurements were carried out at 25°C; temperature control was achieved with a Peltier element. The samples were exposed to X-rays 3 times for 3 minutes each. The two-dimensional scattering patterns were integrated into a one-dimensional scattering function  $I(q)$ . This scattering curve is a function of the magnitude of the scattering vector  $q = (4\pi/\lambda)\sin(\theta/2)$ , where  $\theta$  is the total scattering angle. The absolute intensity was calculated using water as a secondary standard.[1] The one dimensional scattering curves were further treated using the GIFT program.[2-4] A size distribution of spheres weighted by volume was calculated by indirect Fourier transformation.

#### *ζ-potential*

For ζ-potential analysis, a Zeta Plus 90Plus Instrument from Brookhaven (Holtsville, NY, USA) was used. The electrophoretic mobility,  $\mu$ , was measured and transformed into ζ-potential according the Smochulowski equation[5] ( $\zeta=4\eta\pi\mu/\varepsilon$ ), where  $\zeta$  gives the ζ-potential [mV], the electrophoretic mobility is given by  $\mu$  [m<sup>2</sup> s<sup>-1</sup> V<sup>-1</sup>],  $\varepsilon$  is the dielectric constant of the dispersing medium [A s V<sup>-1</sup> m<sup>-1</sup>] and  $\eta$  the solvent viscosity [kg m<sup>-1</sup> s<sup>-1</sup>]. The pH series were titrated with 0.1 M NaOH and 0.1 M HCl, respectively (**Fig. S3**).

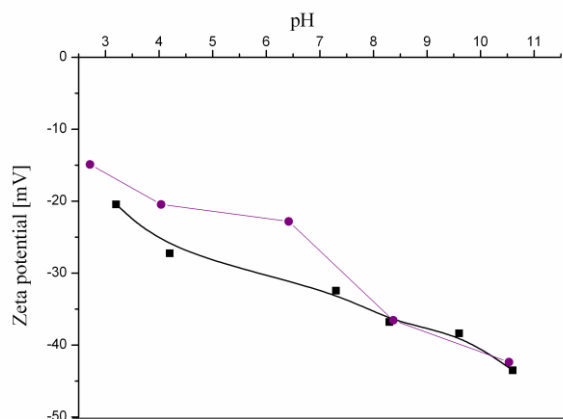


**Figure S3.** Zeta potential in dependence of the pH value. Black: freshly prepared AgNPs; purple: after four weeks of exposure to ambient atmosphere.

#### *Quartz Crystal Microbalance with dissipation (QCM-D)*

A QCM-D instrument (model E4) from Q-Sense, Gothenburg, Sweden was used. The instrument simultaneously measures changes in the resonance frequency ( $\Delta f_n$ ) and energy dissipation ( $\Delta D$ ) when the mass of an oscillating piezoelectric crystal changes upon increase/decrease in the mass of the crystal surface due to the added/deducted mass. Dissipation refers to the frictional losses that lead to damping of the oscillation depending on the viscoelastic properties of the material. For a rigid adsorbed layer that is fully coupled to the oscillation of the crystal,  $\Delta f_n$  is given by the Sauerbrey equation (1)

$$\Delta m = C \frac{\Delta f_n}{n} \quad (1)$$

where  $\Delta f_n$  is the observed frequency shift,  $C$  is the Sauerbrey constant ( $-17.7 \text{ ng Hz}^{-1} \text{ cm}^{-2}$  for a 5 MHz crystal),  $n$  is the overtone number ( $n = 1, 3, 5$ , etc.), and  $\Delta m$  is the change in mass of the crystal due to the adsorbed layer. The mass of a soft (i.e. viscoelastic) film is not fully coupled to the oscillation and the Sauerbrey relation is not valid since energy is dissipated in the film during the oscillation. The damping (or dissipation) ( $D$ ) is defined as

$$D = \frac{E_{diss}}{2\pi E_{stor}} \quad (2)$$

where  $E_{diss}$  is the energy dissipated and  $E_{stor}$  is the total energy stored in the oscillator during one oscillation cycle. For the data analysis in this study, the changes in the third overtone's frequency and dissipation ( $\Delta f_3$ ,  $\Delta D_3$ ) were determined. Dissipation remains in the rigid regime in all experiments described in this paper, therefore the Sauerbrey equation can be applied without any restrictions.

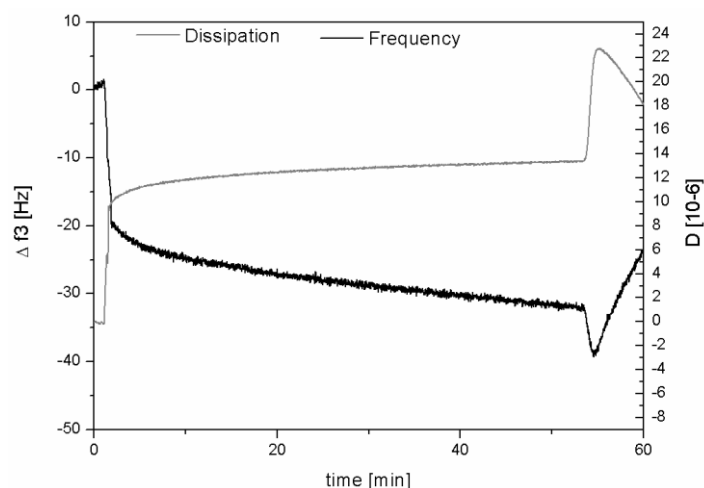


**Figure S4.** QCM-D-data of the adsorption of S-Chi@Ag on CMC using the EDC route.

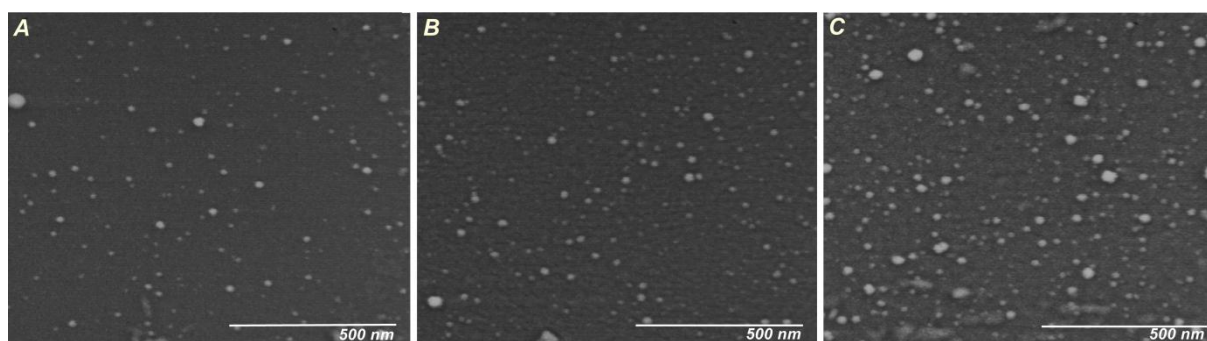


**Figure S5.** SEM images of Ag@S-Chi immobilized on CMC surfaces using different approaches. A: via EDC, B: via EDC/NHS, C: via PEI.

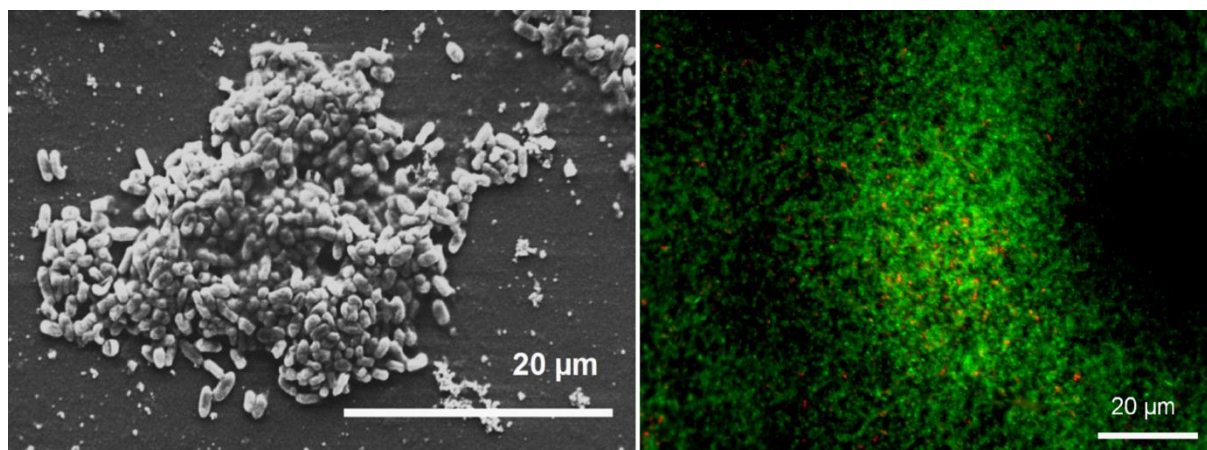


**Figure S6.** Left: SEM image of a CMC surface incubated with *E. coli* MG 1655 [R1-16]. Right: Overlay of fluorescent images from live/dead KIT of a CMC surface after exposure to *E. coli*. The green color indicates that mainly alive bacteria are present.

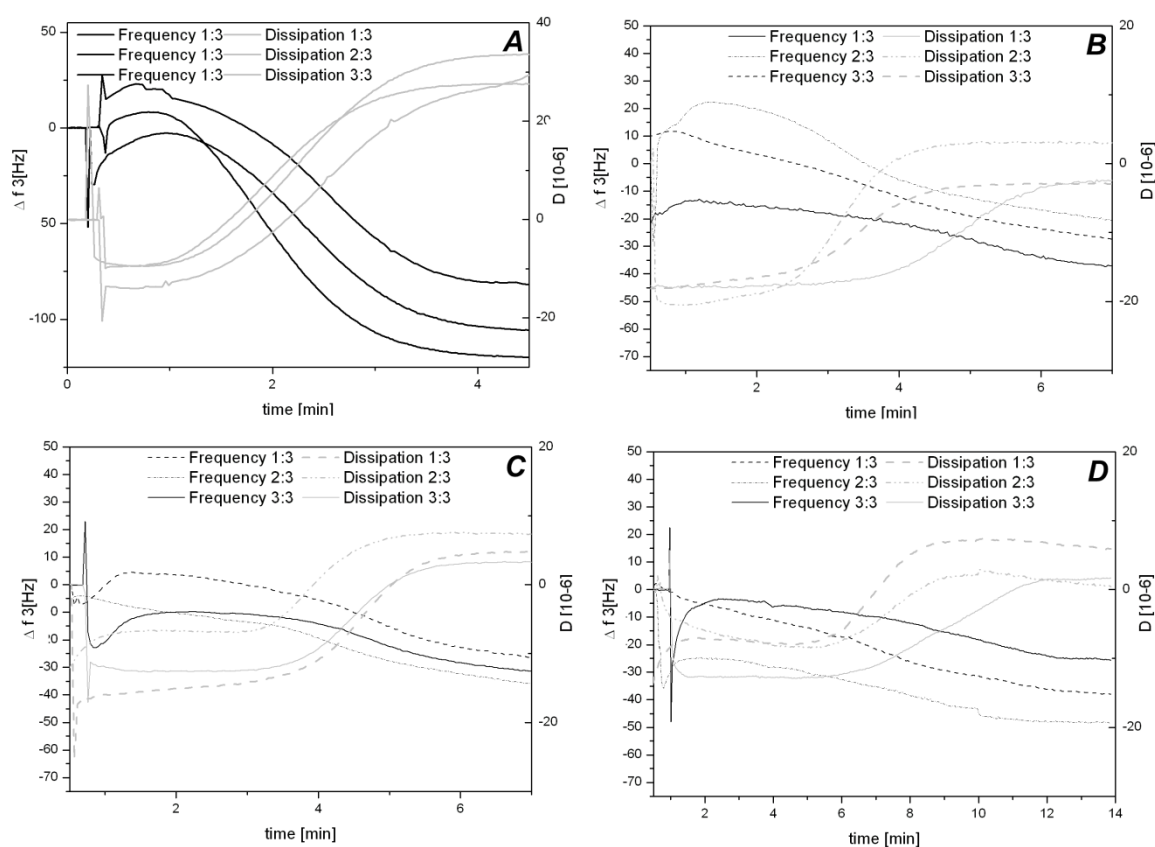


**Figure S7.** Individual curves for the determination of total coagulation times of citrated blood plasma on differently treated surfaces using QCM-D. A: CMC, B: S-Chi@Ag via EDC on CMC, C: S-Chi@Ag via EDC/NHS on CMC, D: S-Chi@Ag via PEI on CMC.

## References

- [1] O. Glatter, J. Appl.Cryst. 1979, 12, 166.
- [2] O. Glatter, J. Appl.Cryst. 1977, 10, 415.
- [3] O. Glatter, J. Appl.Cryst. 1980, 13, 7.
- [4] B. Weyerich, J. Brunner-Popela, O. Glatter, J. Appl.Cryst. 1999, 32, 197.
- [5] M. Smoluchowski, Handbuch der Elektrizität und des Magnetismus, Vol. 2, Barth-Verlag, Leipzig, 1921.